Math Geosci (2012) 44:27–46
DOI 10.1007/s11004-011-9366-1

Co-simulating Total and Soluble Copper Grades in an Oxide Ore Deposit

Xavier Emery

Received: 18 April 2011 / Accepted: 10 September 2011 / Published online: 22 October 2011

Abstract In oxide copper deposits, the acid soluble copper represents the fraction of total copper recoverable by heap leaching. Two difficulties often complicate the joint modeling and simulation of total and soluble copper grades: the inequality constraint linking both grade variables and the sampling design for soluble copper grade, which may be preferential and cause biases in sample statistics. A methodology is presented in order to accurately estimate the total and soluble copper grade bivariate distribution, based on an explicit modeling of the conditional distributions of soluble copper grade. Co-simulation is then realized by converting the copper grades into Gaussian random fields, through stepwise conditional transformation, and by fitting a coregionalization model while accounting for the preferential sampling design. The proposed approach is illustrated through an application to an ore deposit located in northern Chile.

Keywords Inequality constraint · Preferential sampling · Conditional transformation · Conditional simulation · Conditional variogram

1 Introduction

In oxide copper deposits, when the mined material is processed by heap leaching, the total copper grade does not correspond to the actually recovered grade, as the recoveries of the different oxide minerals vary to a great extent (Parkinson and Bhappu 1995; Razavizadeh and Afshar 2008). Consequently, the mineral resources evaluation, giving the basis for economic analysis, mine design and mine planning, should consider

X. Emery (✉)
Department of Mining Engineering, University of Chile, Santiago, Chile
e-mail: xemery@ing.uchile.cl

X. Emery
Advanced Mining Technology Center, University of Chile, Santiago, Chile

not only the total copper grade, but also the acid soluble copper grade, which corresponds to the fraction of total copper recoverable by heap leaching. In the scope of geostatistical modeling, this leads to the problem of jointly estimating or jointly simulating the total and soluble copper grades.

One difficulty for co-estimation or co-simulation is the inequality constraint between both grade variables, as soluble copper grade is always less than or equal to total copper grade. Several approaches have been proposed to reproduce such a constraint, e.g.: quadratic programming (Mallet 1980), constrained interpolation functions (Dubrule and Kostov 1986), stepwise conditional transformation (Leuangthong and Deutsch 2003) or change to variables free of inequality constraints (Emery et al. 2004).

A second difficulty commonly met in practice arises from the unequal sampling of total and soluble copper grades. Typically, total copper is assayed prior to deciding whether or not soluble copper is worth being assayed. Such a preferential sampling leads to biases in the sample distribution of soluble copper grade, as missing data are likely to correspond to low grades. Attempts to deal with preferential sampling include the use of declustering techniques for calculating sample histograms and variograms (Goovaerts 1997, p. 79; Richmond 2002; Emery and Ortiz 2005, 2007), debiasing techniques based on the dependence relationship with a secondary variable (Deutsch et al. 1999; Pyrcz and Deutsch 2003), removal of clustered data in order to achieve a non-preferential sampling (Olea 2007), subdivisions into more homogeneously sampled subdomains (Guan and Afshartous 2007), and use of likelihood-based inference methods (Diggle et al. 2010).

In the following, the problem of modeling the joint distribution of total and soluble copper grades and of co-simulating these grades is addressed. The proposed approach follows the works of Pyrcz and Deutsch (2003) for debiasing the sample distribution of soluble copper grade, based on its relationship with total copper grade, and of Leuangthong and Deutsch (2003) for transforming the total and soluble copper grades into jointly Gaussian random fields. However, rather than working with empirical distributions, which requires binning the data, an explicit modeling of the univariate and bivariate distributions of total and soluble copper grades will be undertaken, through the use of gamma and beta distributions. Another issue that will be examined relates to variogram analysis in the presence of a preferential sampling, implying biased sample variograms. The methodology will be presented together with a case study corresponding to a Chilean copper deposit.

2 Presentation of Case Study

2.1 Original Data Set

The data set under consideration consists of 15,622 drill hole samples, composited at 1.5 meter, from the oxide zone of a porphyry copper deposit located in northern Chile. Acid soluble copper mainly occurs in the form of chrysocolla, atacamite, malaquite and pseudo-malaquite, but a proportion of the copper mineralization is in an acid insoluble form due to the presence of copper wad and copper pitch. Total and

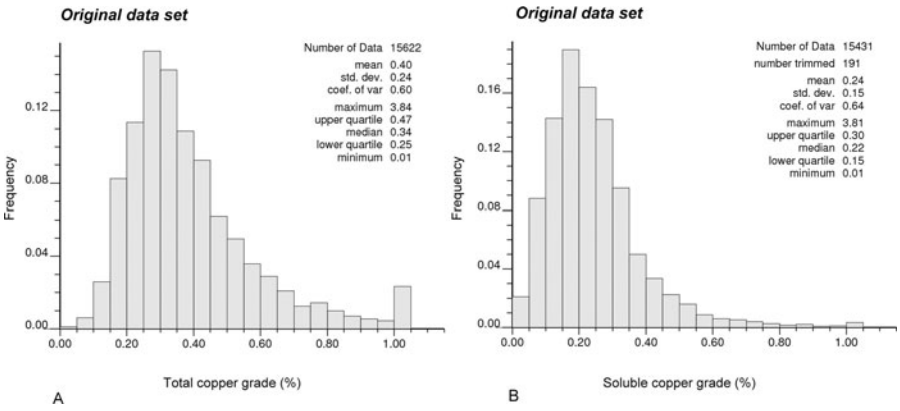

Fig. 1 Histograms of (**A**), total copper grade and (**B**), soluble copper grade (original data set)

soluble copper grades have been assayed in almost all the samples, so that the sample distributions of both grades can be assumed representative of the entire deposit (Fig. 1; Table 1). In the following sections, the original grade values are adjusted by a constant scale factor in order to preserve the confidentiality of the data.

2.2 Preferential Sampling

In order to test the accuracy of the proposed methodology, a new data set is generated, by purposely removing 85% of the soluble copper grade information at the data for which the total copper grade is less than 0.3%. Accordingly, the sample distribution of soluble copper grade in this new data set is biased with respect to the true underlying distribution (Fig. 2, Table 1).

3 Modeling Total and Soluble Copper Grade Distributions

3.1 Univariate Distribution of Total Copper Grade

Since the sampling of total copper grade is not preferential, the distribution of this variable can be inferred without bias from the sample distribution. In practice, it can be modeled through a transformation to a given theoretical distribution (Chilès and Delfiner 1999, p. 406). In the following, a standard gamma distribution is considered, the density of which is defined on $\mathbb{R}_+$ as

$$\forall y \in \mathbb{R}_+, \quad g_\alpha(y) = \frac{1}{\Gamma(\alpha)} e^{-y} y^{\alpha-1} \tag{1}$$

where Γ is the Euler gamma function and $\alpha > 0$ is a shape parameter that determines the skewness of the gamma distribution. This distribution has been chosen because it will allow the construction of a bivariate model for the total and soluble copper grades that is consistent with the inequality constraint between these two grades (Sect. 3.2).

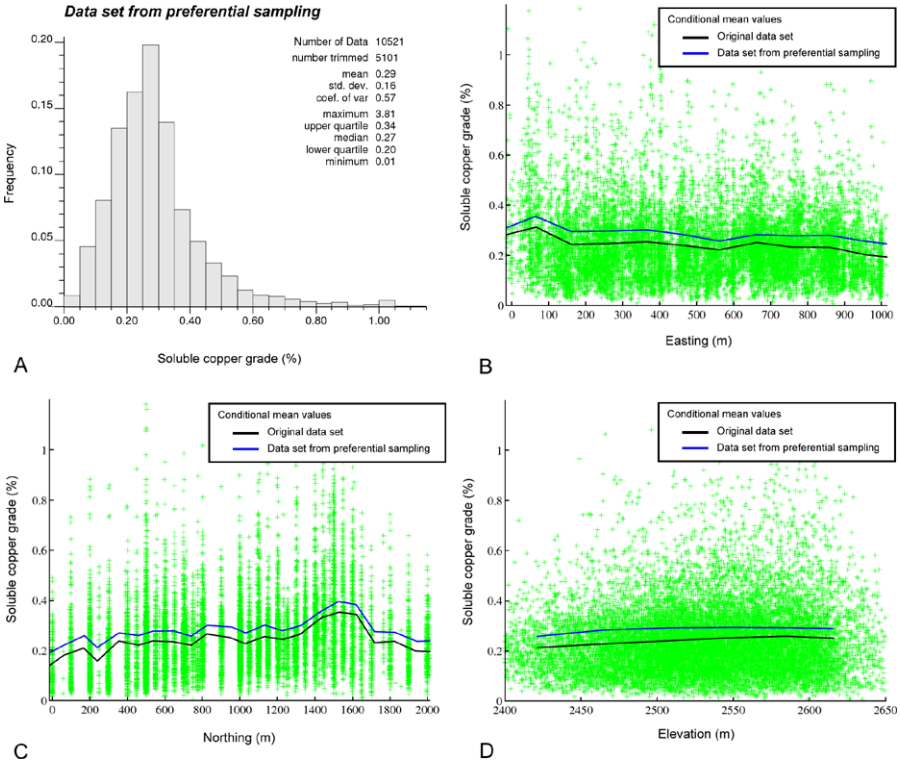

Fig. 2 (**A**) Histogram of soluble copper grade for biased data set. (**B**), (**C**), and (**D**), scatter diagrams of soluble copper grades vs. coordinates (conditional mean curves are superimposed, for both the original and biased data sets)

Table 1 Basic statistics of copper grade data

Variable	Number of data	Minimum (%)	Maximum (%)	Mean (%)	Standard deviation (%)	Correlation with total copper grade
Total copper grade (original data set)	15,622	0.013	3.836	0.396	0.236	
Soluble copper grade (original data set)	15,431	0.007	3.808	0.244	0.155	0.732
Soluble copper grade (preferential data set)	10,521	0.014	3.808	0.289	0.165	0.667

Such a constraint cannot be reproduced when considering the well-known bivariate Gaussian model.

Let Z_1 denote the total copper grade and Y_1 its gamma transform

$$Z_1 = \phi_\alpha(Y_1), \tag{2}$$

where ϕ_α is a non-decreasing function called gamma anamorphosis. It can be determined experimentally via expansions into Laguerre polynomials (Hu and Lantuéjoul 1988) or via the definition of a transformation table (Emery 2006).

3.2 Bivariate Distribution of Total and Soluble Copper Grades

Let now Z_2 be the soluble copper grade and define Y_2 as

$$Z_2 = \phi_\alpha(Y_2). \tag{3}$$

The same anamorphosis function ϕ_α has been applied to Z_1 and Z_2 in order to preserve the inequality constraint between the transformed random fields Y_1 and Y_2. Indeed, because ϕ_α is a non-decreasing function, one has $0 \leq Y_2 \leq Y_1$.

The joint distribution of total and soluble copper grades will be determined by specifying a bivariate model between Y_1 and Y_2. To this end, let us write

$$Y_2 = BY_1, \tag{4}$$

where B is a random variable with outcomes in $[0, 1]$. As a particular case, if B is a beta random variable independent of Y_1 and with parameters $\{a, b\}$ such that $a + b = \alpha$, then Y_2 is a standard gamma random variable with shape parameter a and the joint density of (Y_1, Y_2) is (McKay 1934; Yeo and Milne 1991)

$$\forall y_1 \in \mathbb{R}_+, \forall y_2 \in [0, y_1], \quad f_{a,b}(y_1, y_2) = \frac{y_2^{a-1}(y_1 - y_2)^{b-1}e^{-y_1}}{\Gamma(a)\Gamma(b)}. \tag{5}$$

A more general model consists of the assumption that, conditionally to $Y_1 = y_1$, B has a beta distribution with parameters

$$\begin{cases} a = h_1(y_1), \\ b = h_2(y_1) \end{cases} \tag{6}$$

for some positive functions h_1 and h_2. Consequently, the raw moments of Y_2 conditionally to $Y_1 = y_1$ are

$$\begin{aligned} \forall n > 0, \quad \mu_n(y_1) &= E\big(Y_2^n | Y_1 = y_1\big) \\ &= E\big(B^n | Y_1 = y_1\big) y_1^n \\ &= \frac{\Gamma(h_1(y_1) + n)\Gamma(h_1(y_1) + h_2(y_1))}{\Gamma(h_1(y_1) + h_2(y_1) + n)\Gamma(h_1(y_1))} y_1^n. \end{aligned} \tag{7}$$

Functions h_1 and h_2 can be determined by considering the first two moments, leading to

$$\begin{cases} h_1 = \frac{\mu_1(\mu_1 - \mu_2)}{\mu_2 - \mu_1^2}, \\ h_2 = \frac{(1-\mu_1)(\mu_1 - \mu_2)}{\mu_2 - \mu_1^2} \end{cases} \tag{8}$$

and by replacing μ_1 and μ_2 by the experimental regressions of Y_2 upon Y_1 and of Y_2^2 upon Y_1, respectively. These regressions are assumed to be unbiased estimates of

the conditional moments μ_1 and μ_2, insofar as there is no preferential sampling of soluble copper grade for a given total copper grade, i.e., the sample distribution of Y_2 conditional to $Y_1 = y_1$ is assumed representative of the theoretical distribution of $\{Y_2|Y_1 = y_1\}$.

Accordingly, the steps to determine the model parameters are the following.

1. Choose a value for the shape parameter α.
2. Transform the total copper grade data into gamma distributed data (gamma scores) with shape parameter α and determine the gamma anamorphosis function ϕ_α (see (2)).
3. Use the inverse function ϕ_α^{-1} to transform the available soluble copper grade data into data on Y_2 (see (3)).
4. Determine the experimental regression curves $\hat{\mu}_1$ and $\hat{\mu}_2$ of Y_2 and Y_2^2 upon Y_1.
5. Substitute $\hat{\mu}_1$ and $\hat{\mu}_2$ for μ_1 and μ_2 in (8), in order to obtain estimates $\hat{h}_1$ and $\hat{h}_2$ of functions h_1 and h_2.
6. Fit a model to $\hat{h}_1$ and $\hat{h}_2$, using known basis functions, e.g., exponential functions. A practical difficulty arises if soluble copper grades are strongly under-sampled for low total copper grades: because of the scarcity of data, $\hat{h}_1(y_1)$ and $\hat{h}_2(y_1)$ may be poor estimates of $h_1(y_1)$ and $h_2(y_1)$ for low values of y_1, so that the fit mainly relies on extrapolating the behavior observed for higher values of y_1. If the fit is deemed unsatisfactory or too complex, the shape parameter α chosen at Step 1 can be changed.
7. Numerically determine the joint and marginal distributions of (Z_1, Z_2). To this end, generate a large set of realizations of Y_1, then, for each realization, generate a realization of B (see (6)), obtain a realization of Y_2 (see (4)) and back-transform the pair (Y_1, Y_2) into (Z_1, Z_2) (see (2) and (3)).

3.3 Application

For the application to the case study presented in Sect. 2, a shape parameter $\alpha = 4$ has been chosen for the transformation of the total copper grade. This parameter corresponds to a moderately skewed gamma probability density function, similar in shape to the original total copper grade distribution (Fig. 1(A), 3(A)). The gamma anamorphosis function ϕ_α (see (2)) has been determined following the methodology presented by Emery (2006). From the total copper grade sample distribution, an empirical transformation table is calculated first, then a piecewise linear interpolation is used for determining ϕ_α at any intermediate value, while exponential functions are used for tail extrapolation (Fig. 3(B)).

Provided with the gamma anamorphosis function ϕ_α, the soluble copper grade data are transformed according to (3) and the scatter diagrams of Y_1 and Y_2 (Fig. 4(A)) and of Y_1 and Y_2^2 (Fig. 4(B)) are constructed. The experimental regressions $\hat{\mu}_1$ and $\hat{\mu}_2$ of these scatter diagrams are used to estimate functions h_1 and h_2 (see (8)), which are finally fitted with exponential functions (Fig. 4(C), 4(D))

$$\forall y \in \mathbb{R}_+, \quad \begin{cases} h_1(y) = \exp(1.3964 - 0.1068y), \\ h_2(y) = \exp(1.0542 - 0.1092y). \end{cases} \tag{9}$$

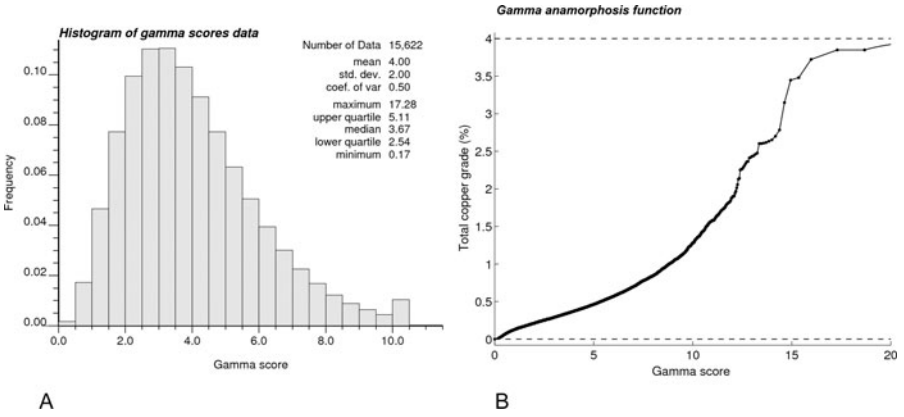

Fig. 3 (**A**) Distribution of gamma scores data of total copper grade (variable Y_1); (**B**) experimental (*dots*) and modeled (*solid line*) gamma anamorphosis function

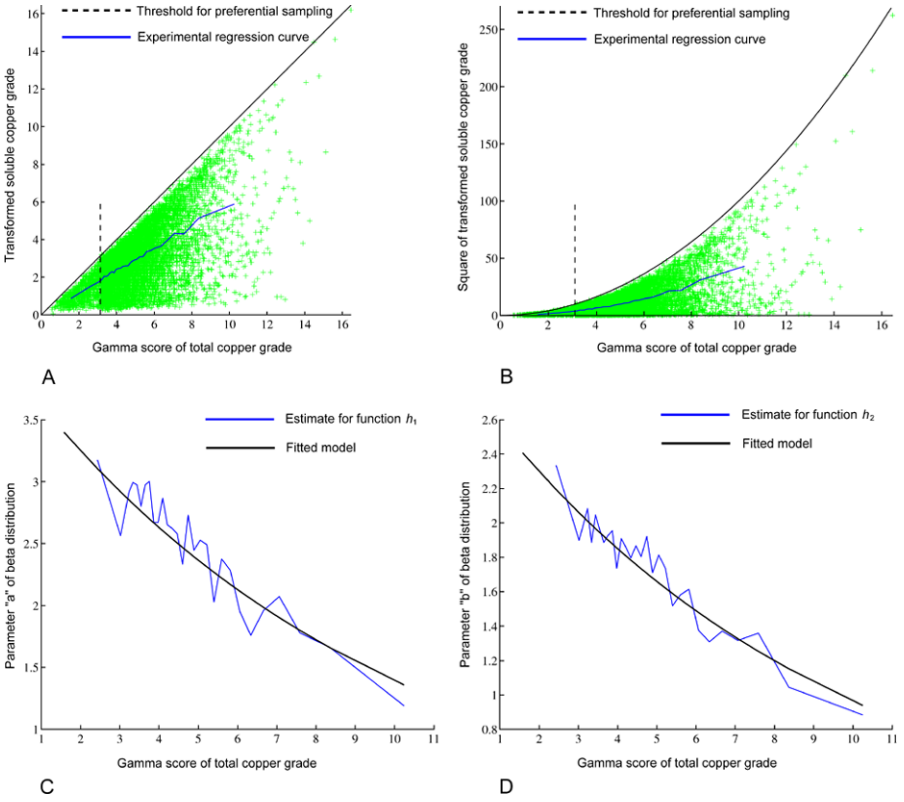

Fig. 4 Scatter diagrams of gamma scores data of total copper grade (Y_1) versus (**A**), transformed soluble copper grade (Y_2) and (**B**), squared transformed soluble copper grade (Y_2^2). Experimental curves and fitted models for (**C**), function h_1 and (**D**), function h_2

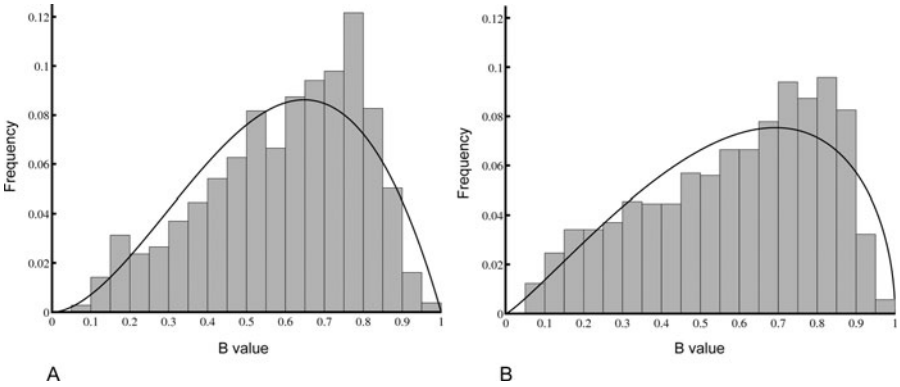

Fig. 5 Distributions of $B = Y_2/Y_1$ conditional to (**A**), $Y_1 = 3.35$ and (**B**), $Y_1 = 5.80$. Histograms correspond to sample conditional distributions (tolerances on the values of Y_1 have been used in order to get about 1000 data per histogram). Superimposed *solid lines* are the theoretical beta distributions, rescaled by a factor 20 corresponding to the number of histogram classes

The fit is validated by comparing the sample distribution of $B = Y_2/Y_1$ conditional to $Y_1 = y_1$ with the beta distribution of parameters $h_1(y_1)$ and $h_2(y_1)$, for a few selected values of y_1 (Fig. 5).

Having fitted functions h_1 and h_2, one can simulate a large number of realizations of total and soluble copper grades (Sect. 3.2), giving numerical representations of the joint and marginal distributions of both grades (Fig. 6). The marginal distribution of soluble copper grade so obtained is then compared with the true underlying distribution (inferred from the original data set) through a quantile-quantile plot: it is seen that the modeled distribution almost perfectly matches the true distribution, contrasting with the biased sample distribution obtained after the preferential sampling of soluble copper grade (Fig. 7).

4 Co-simulation of Total and Soluble Copper Grades

4.1 Algorithm

The co-simulation of total and soluble copper grades conditional to the available drill hole data values is now addressed. To avoid simulating random fields linked by an inequality constraint ($Z_2 \leq Z_1$), a change of variables will be considered. It relies on the pair of variables (Y_1, B) defined in (4), for which co-simulation can be done under the well-known multi-Gaussian model (Verly 1983; Chilès and Delfiner 1999, p. 381).

The steps for co-simulation are as follows.

1. Transform the total and soluble copper grade data into data on Y_1 and Y_2 (see (2)–(3)).
2. Calculate $B = Y_2/Y_1$ at the locations where both the total and soluble copper grades are sampled (see (4)). Unlike Y_1, B is not known at all the data locations because of the preferential sampling of soluble copper grade.

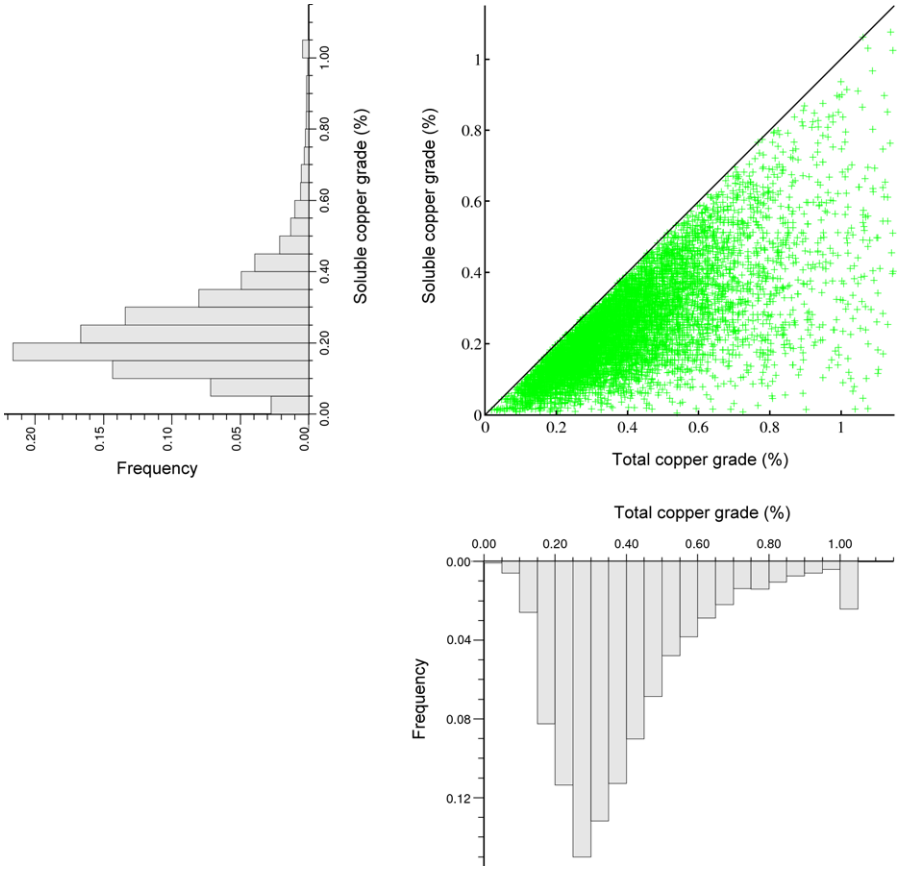

Fig. 6 Modeled bivariate and marginal distributions for total and soluble copper grades, calculated on the basis of 15,000 realizations

3. Based on the distributions of Y_1 (see (1)) and B (see (6)), transform the data on Y_1 and B into data with standard Gaussian distributions (normal scores). Denoting by G, G_α and $G_{a,b}$ the standard Gaussian, gamma and beta cumulative distribution functions, respectively, the Gaussian transforms are defined by

$$\begin{cases} T_1 = G^{-1} \circ G_\alpha(Y_1), \\ T_2 = G^{-1} \circ G_{h_1(Y_1),h_2(Y_1)}(B). \end{cases} \tag{10}$$

Note that the transformation function used for B depends on Y_1. It is comparable to the stepwise conditional transformation proposed by Leuangthong and Deutsch (2003), except that here the use of theoretical distribution models (gamma for Y_1 and beta for B) avoids the problems caused by the discretization of the empirical distributions (banding effect) and by the missing B-values. Moreover, the resulting Gaussian random fields T_1 and T_2 are not assumed to be uncorrelated for the zero lag separation vector.

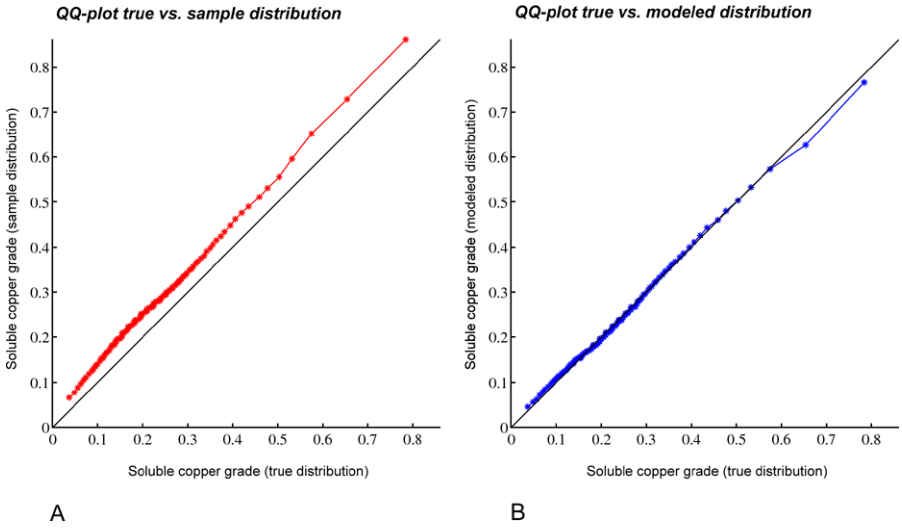

Fig. 7 Quantile–quantile plot of true soluble copper grade distribution (original data set) versus (**A**), biased sample distribution and (**B**), modeled distribution

4. Calculate the sample direct and cross variograms of T_1 and T_2 and fit a coregionalization model.
5. Co-simulate (T_1, T_2) at the target grid locations, conditionally to the information at the data locations. This step amounts to traditional conditional co-simulation in the multi-Gaussian context; it can be performed by any Gaussian simulation algorithm, e.g., sequential, spectral or turning bands simulation (Goovaerts 1997, p. 388; Chilès and Delfiner 1999, p. 460; Lantuéjoul 2002, p. 183; Emery 2008).
6. Back-transform the simulated fields (T_1, T_2) into (Y_1, B) (see (10)), then into (Z_1, Z_2) (see (2)–(4)).

4.2 Variogram Analysis

Let us assume that the random fields (T_1, T_2) defined in (10) are stationary and jointly Gaussian. Due to the preferential sampling of the soluble copper grade, depending on whether or not the total copper grade is above threshold $z_1 = 0.3\%$, T_2 is unknown at some data locations and its sample variogram might be a biased estimate of its prior variogram. A few examples of such biases occurring in the presence of a preferential sampling are presented in Appendix.

To solve this issue, a trial-and-error procedure is proposed, through the following steps.

1. Calculate the sample variogram of T_1, which provides an unbiased estimate of the prior variogram of this random field.
2. Select the subset of data locations at which the total copper grade is greater than z_1 (above this threshold, almost all the data carry information on the total and soluble copper grades). This subset can equivalently be defined by selecting the data for

which T_1 is greater than a threshold t_1 such that $z_1 = \phi_\alpha \circ G_\alpha^{-1} \circ G(t_1)$ (see (2), (10)).

3. Using the normal scores data at the selected data locations, calculate the sample direct and cross variograms of T_1 and T_2, for given lag separation vectors $\{\mathbf{h}_k, k = 1, \ldots, K\}$. These sample variograms are unbiased estimates of the variograms of the Gaussian random fields T_1 and T_2 conditioned to $T_1 > t_1$. Hereafter, they will be referred to as "conditional variograms", as opposed to the prior (non-conditional) variograms of T_1 and T_2.
4. Propose a coregionalization model for T_1 and T_2, i.e., direct and cross variogram models. For the random field T_1, the direct variogram model should be chosen in order to fit the sample variogram calculated at Step 1.
5. For each lag separation vector $\mathbf{h}_k$ where the sample conditional variograms have been calculated:
   (i) Generate a large number of realizations of the Gaussian random vector $(T_1(\mathbf{0}), T_2(\mathbf{0}), T_1(\mathbf{h}_k), T_2(\mathbf{h}_k))$. The LU triangular decomposition of the covariance matrix algorithm (Davis 1987) can be used at this stage.
   (ii) Discard the realizations for which $T_1(\mathbf{x}) \leq t_1$ at $\mathbf{x} = \mathbf{0}$ or $\mathbf{x} = \mathbf{h}_k$.
   (iii) With the remaining realizations, calculate the direct and cross variograms of T_1 and T_2 for the lag separation vector $\mathbf{h}_k$, which approximate the theoretically expected conditional variograms. Although the conditional direct variogram of T_1 can be calculated analytically as a function of the prior variogram (see (18) in Appendix), a numerical approach has been preferred here because analytical calculations are cumbersome for the conditional direct variogram of T_2 and cross variogram between T_1 and T_2.
6. Compare the sample and theoretically expected conditional variograms obtained at Steps 3 and 5. If the fit is not satisfactory, go back to Step 4.

The above procedure can be simplified if T_1 and T_2 are independent random fields. In such a case, the restriction to a subset of data locations depending on the values of T_1 (Step 2) does not provoke any bias on the distribution of T_2, in particular on its variogram. In other words, provided that T_1 and T_2 are independent, the conditional variogram of T_2 is the same as its prior variogram. The variogram fitting procedure can therefore be achieved by fitting prior variogram models to the sample direct variograms calculated by using all the available data, without caring about the preferential sampling.

4.3 Application

The total and soluble copper grade data are transformed into normal scores data on (T_1, T_2). By considering only the data with a total copper grade greater than $z_1 = 0.3\%$, the sample conditional variograms of (T_1, T_2) are then calculated along the horizontal and vertical directions, recognized as the main directions for anisotropy and variogram modeling. The cross variogram takes low values (between -0.05 and 0.10), indicating that the random fields T_1 and T_2 are poorly correlated (Fig. 8). Accordingly, these two random fields are assumed independent and a separate modeling of their direct variogram is undertaken (Fig. 9(A), 9(B)). The following prior variogram models, nesting nugget, exponential and spherical structures with a geometric anisotropy between the horizontal and the vertical directions, are found

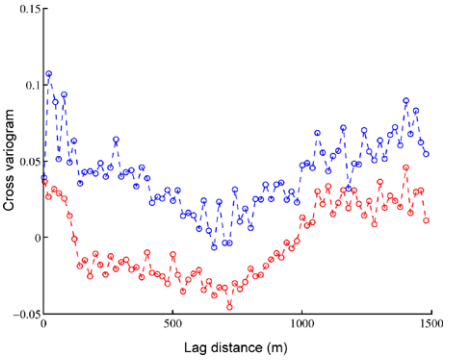

Fig. 8 Sample cross variogram of normal scores data on T_1 and T_2, along the horizontal (*blue*) and vertical (*red*) directions, calculated by using the data with total copper grade above 0.3%

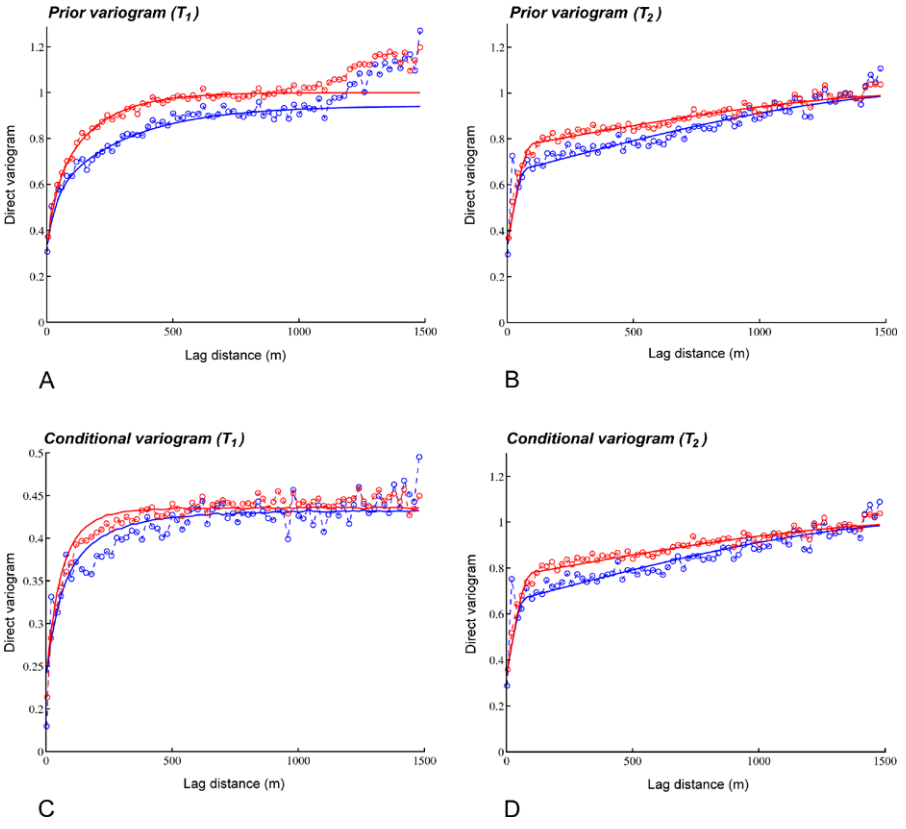

Fig. 9 Direct variograms of normal scores data on T_1 and T_2, along the horizontal (*blue*) and vertical (*red*) directions, calculated with (**A**), (**B**), all the available data from the biased data set, (**C**), (**D**), the subset of data with total copper grade above 0.3%. Sample variograms are indicated with *circles* and *dashed lines*, models with *solid lines*

$$\begin{cases} \gamma_{T_1} = 0.32\text{nugget} + 0.22\,\text{exp}(100\text{ m}, 100\text{ m}) \\ \qquad\quad + 0.4\,\text{exp}(900\text{ m}, 500\text{ m}) + 0.06\,\text{exp}(\infty, 600\text{ m}), \\ \gamma_{T_2} = 0.33\text{nugget} + 0.32\,\text{sph}(75\text{ m}, 100\text{ m}) \\ \qquad\quad + 0.11\,\text{sph}(1800\text{ m}, 100\text{ m}) + 0.24\,\text{sph}(1800\text{ m}, 1800\text{ m}), \end{cases} \tag{11}$$

where the distances into brackets indicate the horizontal and vertical ranges, respectively.

The fitted models are validated by comparing the sample conditional variograms of T_1 and T_2 (calculated by using the subset of data with a total copper grade greater than 0.3%) with the theoretical conditional variograms (Steps 5–6 of the trial-and-error procedure described in Sect. 4.2). The fitting is excellent for the random field T_2 (Fig. 9(D)), which is explained because the variogram model is unchanged and the sample variogram is almost the same when using the selected subset of data. In contrast, for the random field T_1, a deviation between the sample and modeled conditional variograms is observed, although the fitting remains acceptable (Fig. 9(C)). Given that the conditional variogram of T_1 only depends on its prior variogram and on the assumption of a multivariate Gaussian distribution ((18) in Appendix), the observed deviation can be explained because the actual distribution of the normal scores data on T_1 slightly departs from the distribution of a stationary, standard Gaussian random field.

The independence of T_1 and T_2 indicates that the proposed bivariate model (see (10)) allows to separate a component that only depends on the total copper grade (T_1, which is nothing else than the Gaussian transform of Z_1) and a component that is independent of the total copper grade (T_2) and whose distribution is not affected by the preferential sampling pattern. This preferential sampling, however, has an impact on the soluble copper grade distribution (in particular, on its variogram), insofar as Z_2 depends on both T_1 and T_2 (see (3), (4), and (10)).

Having fitted and validated the coregionalization model of the Gaussian random fields T_1 and T_2, the turning bands algorithm (Emery and Lantuéjoul 2006) is used to generate 100 point-support conditional realizations of these two random fields. The size of the domain targeted for co-simulation is 1000 m × 1500 m × 150 m and the grid mesh has been set to 2.5 m × 2.5 m × 5 m. After back-transformation, one obtains 100 point-support conditional realizations of the total and soluble copper grades, which are finally regularized to a block support of 10 m × 10 m × 10 m. The maps of the first realization and of the average of 100 realizations for a given elevation are displayed in Fig. 10.

Table 2 gives estimates of the resources that can be recovered above given cut-offs associated with total copper grade: fraction of tonnage, mean grades above cut-off and solubility ratio, defined as the quotient between soluble and total copper grades. These estimates have been obtained by averaging the recoverable resources calculated on each realization. The overall mean soluble copper grade (mean grade above a zero cut-off grade) is 0.237%, very close to the mean soluble copper grade of the original data set (0.243%). The importance of using the realizations individually for estimating the copper resources is clear from Fig. 10, insofar as the expected grades obtained by averaging the realizations yield smooth maps and therefore lead to biased grade-tonnage curves, as illustrated in Fig. 11 for the tonnage and mean soluble copper grades above cut-off.

The total and soluble copper grade realizations can also be used for mine planning and for decision-making. For instance, assume that each mined block can have three possible destinations: flotation plant if the total copper grade is above 0.5% and the solubility ratio is less than 70%, dump if the soluble copper grade is less than 0.25%,

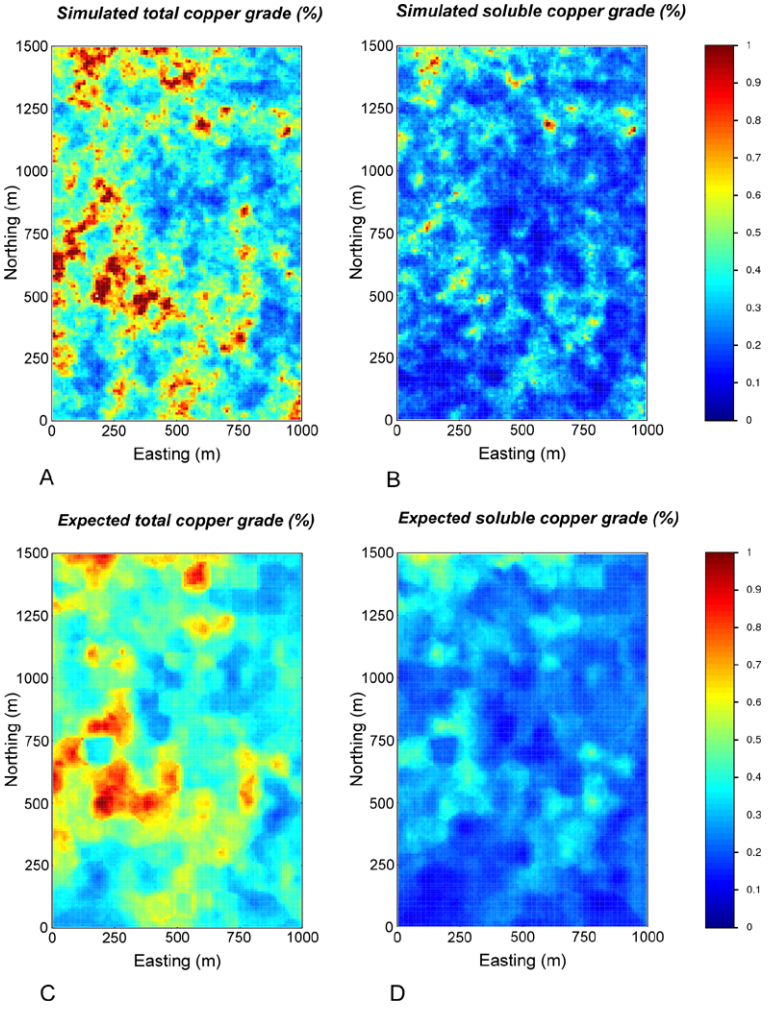

Fig. 10 (**A**), (**B**) Maps of simulated total and soluble copper grades for realization #1. (**C**), (**D**) Maps of expected total and soluble copper grades (average of 100 realizations)

and heap leaching otherwise. The realizations can be used to calculate the probability of each destination for each block and to assign the most probable destination (Table 3); such a classification cannot be performed when separately simulating total and soluble copper grades, but only through a joint simulation of these grades.

5 Conclusions

The quantification of total and soluble copper grade resources is a recurrent problem in the evaluation of oxide ore deposit. The main difficulties arise from the functional dependence (inequality constraint) between the grade variables and, regarding soluble

Table 2 Tonnages, mean grades and mean solubility ratios for different cut-off grades, calculated from 100 block-support conditional realizations

Cut-off grade (% total copper)	Fraction of tonnage	Mean total copper grade (%)	Mean soluble copper grade (%)	Mean solubility ratio
0.00	1.000	0.406	0.237	0.599
0.10	0.999	0.406	0.237	0.599
0.20	0.951	0.418	0.244	0.599
0.25	0.857	0.439	0.254	0.595
0.30	0.712	0.472	0.270	0.589
0.35	0.557	0.513	0.288	0.573
0.40	0.419	0.559	0.308	0.560
0.45	0.307	0.608	0.328	0.547
0.50	0.222	0.660	0.349	0.535
0.55	0.160	0.713	0.370	0.524
0.60	0.115	0.767	0.391	0.515
0.65	0.084	0.821	0.412	0.507
0.70	0.061	0.876	0.433	0.499
0.80	0.033	0.986	0.475	0.486
0.90	0.019	1.097	0.518	0.475
1.00	0.011	1.210	0.560	0.466

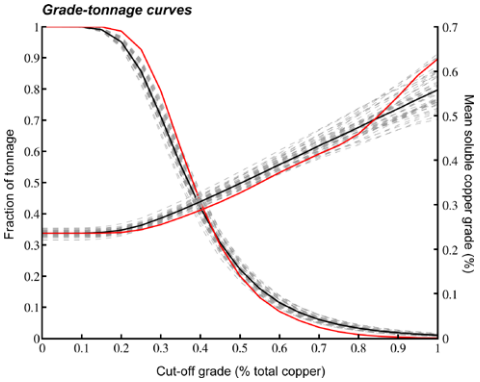

Fig. 11 Fractions of tonnage and mean soluble copper grades above cut-off grades, calculated on each realization (*dashed lines*) and averaged over all the realizations (*solid black line*). Grade-tonnage curves calculated by using the average of the realizations are indicated with *solid red lines*

copper grade, from the stochastic dependence between the grade and the sampling design, insofar as the soluble copper grade is generally not assayed at the samples with low total copper grade (preferential sampling).

A methodology has been presented to face these difficulties and to co-simulate total and soluble copper grades. It consists in modeling the bivariate distribution of total and soluble copper grades, based on their dependence relationship inferred with collocated sample data. The recourse to theoretical distributions (gamma and beta) for this modeling avoids the problems linked to the binning of data when working with empirical distributions, as well as the problems linked to the presence of missing

Table 3 Number of blocks and estimated mean copper grades for each possible destination

Destination	Heap leaching	Flotation	Dump
Number of blocks	39,498	35,896	149,606
Mean total copper grade (%)	0.458	0.622	0.340
Mean soluble copper grade (%)	0.316	0.312	0.197

values for soluble copper grade. The remaining steps are the transformation of total and soluble copper grade data into multi-normally distributed data, joint variogram analysis of the normal scores data, co-simulation of the associated Gaussian random fields and back-transformation into original grades. As shown with the case study, the proposed approach is versatile and of relatively simple use. It can be adapted to more complex distributions than the beta for modeling the ratio variable B, depending on more than two parameters, and to non-stationary models, by considering that these parameters may vary in space, e.g., with the elevation.

Acknowledgements This research was funded by the Chilean Fund for Science and Technology Development, through Fondecyt project 1090013. The author acknowledges the support of the Advanced Laboratory for Geostatistical Supercomputing (ALGES) at the University of Chile.

Appendix: Conditional Variogram

The objective of this appendix is to show that, in the presence of a preferential sampling, the sample variogram may be a biased estimate of the prior variogram model. For the sake of simplicity, consider the case of a single random field $\{Y(\mathbf{x}) : \mathbf{x} \in \mathsf{D}\}$ and of a sampling strategy consisting in locating the samples in areas where the random field takes values above a given threshold y. In this context, the sample variogram is an unbiased estimate of the conditional variogram, defined as

$$\gamma_y(\mathbf{h}) = \frac{1}{2} E\left\{\left[Y(\mathbf{x}+\mathbf{h}) - Y(\mathbf{x})\right]^2 \mid Y(\mathbf{x}+\mathbf{h}) > y, Y(\mathbf{x}) > y\right\}. \tag{12}$$

It is of interest to relate the prior variogram $\gamma(\mathbf{h})$ with the conditional variogram $\gamma_y(\mathbf{h})$. To this end, two stationary random field models (Gaussian and lognormal) will be examined.

First, let us assume that $\{Y(\mathbf{x}) : \mathbf{x} \in \mathsf{D}\}$ is a stationary, standard Gaussian random field. Let g and G be the standard Gaussian probability density function and cumulative distribution function, and g_r the joint density of a standard Gaussian pair with correlation coefficient r. The conditional variogram is

$$\gamma_y(\mathbf{h}) = \frac{1}{2} \frac{\int_y^{+\infty} \int_y^{+\infty} (t-t')^2 g_{1-\gamma(\mathbf{h})}(t,t')\, dt\, dt'}{\int_y^{+\infty} \int_y^{+\infty} g_{1-\gamma(\mathbf{h})}(t,t')\, dt\, dt'}. \tag{13}$$

Let us define the normalized Hermite polynomials $\{H_p, p \in \mathbb{N}\}$ as (Rivoirard 1994, p. 40)

$$\forall p \in \mathbb{N}, \forall t \in \mathbb{R}, \quad H_p(t) = \frac{1}{\sqrt{p!}g(t)} \frac{d^p g(t)}{dt^p} \tag{14}$$

with, in particular

$$\forall t \in \mathbb{R}, \quad H_0(t) = 1, \qquad H_1(t) = -t \quad \text{and} \quad H_2(t) = \frac{1}{\sqrt{2}}\big(t^2 - 1\big). \tag{15}$$

Furthermore, let us define

$$\forall p, q \in \mathbb{N}, \forall y \in \mathbb{R}, \quad S_{pq}(y) = \int_y^{+\infty} H_p(t) H_q(t) g(t)\, dt. \tag{16}$$

$S_{pq}(y)$ can be calculated recursively by using the following identities (Rivoirard 1994, p. 58; Chilès and Delfiner 1999, p. 641)

$$\begin{cases} S_{00}(y) = 1 - G(y), \\ \forall p > 0, \quad S_{0p}(y) = S_{p0}(y) = -\frac{1}{\sqrt{p}} H_{p-1}(y) g(y), \\ \forall p > 0, \forall q > 0, \quad S_{pq}(y) = \sqrt{\frac{p}{q}} S_{p-1q-1}(y) - \frac{1}{\sqrt{q}} H_p(y) H_{q-1}(y) g(y). \end{cases} \tag{17}$$

By expanding g_r into the Hermite polynomials (Chilès and Delfiner 1999, p. 399) and by using (15), it follows from (13) and (16)

$$\begin{aligned} \gamma_y(\mathbf{h}) &= \frac{1}{2} \frac{\sum_{p=0}^{+\infty} [1 - \gamma(\mathbf{h})]^p \int_y^{+\infty} \int_y^{+\infty} (t - t')^2 H_p(t) H_p(t') g(t) g(t')\, dt\, dt'}{\sum_{p=0}^{+\infty} [1 - \gamma(\mathbf{h})]^p \int_y^{+\infty} \int_y^{+\infty} H_p(t) H_p(t') g(t) g(t')\, dt\, dt'} \\ &= \frac{\sum_{p=0}^{+\infty} [1 - \gamma(\mathbf{h})]^p \{\int_y^{+\infty} t^2 H_p(t) g(t)\, dt \int_y^{+\infty} H_p(t') g(t')\, dt' - \big(\int_y^{+\infty} t H_p(t) g(t)\, dt\big)^2\}}{\sum_{p=0}^{+\infty} [1 - \gamma(\mathbf{h})]^p S_{0p}^2(y)} \\ &= \frac{\sum_{p=0}^{+\infty} [1 - \gamma(\mathbf{h})]^p \{(S_{0p}(y) + \sqrt{2} S_{2p}(y)) S_{0p}(y) - S_{1p}^2(y)\}}{\sum_{p=0}^{+\infty} [1 - \gamma(\mathbf{h})]^p S_{0p}^2(y)}. \end{aligned} \tag{18}$$

For numerical calculations, the series in the numerator and denominator can be truncated to a high order, e.g., $p = 200$. In Fig. 12, the conditional variogram γ_y is plotted as a function of the prior variogram γ, for several values of the threshold y ($-\infty$ and the deciles of the standard Gaussian distribution). The conditional variogram is seen to be less than the prior variogram, which indicates that the conditioned Gaussian random field has a smaller variance. Also, because the plotted curves are different from straight lines, the conditional variogram does not have the same shape as the prior variogram. In particular, even if the prior variogram is a non-decreasing function of the lag distance, the conditional variogram at large threshold values (above the median) is likely to present a hole effect.

As a second example, assume that $\{Y(\mathbf{x}) : \mathbf{x} \in \mathsf{D}\}$ is a stationary lognormal random field and that its logarithm is a Gaussian random field with mean m, variance σ^2,

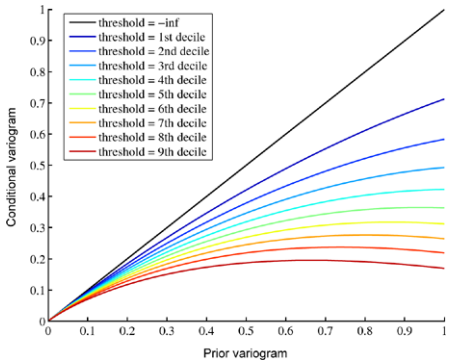

Fig. 12 Conditional variogram as a function of the prior variogram (stationary standard Gaussian random field)

covariance function $C_{\ln}(\mathbf{h})$ and variogram $\gamma_{\ln}(\mathbf{h}) = \sigma^2 - C_{\ln}(\mathbf{h})$. The prior variogram of Y is (Chilès and Delfiner 1999, p. 103)

$$\begin{aligned}\gamma(\mathbf{h}) &= \exp\bigl(2m+\sigma^2\bigr)\bigl[\exp\bigl(\sigma^2\bigr)-1\bigr] - \exp\bigl(2m+\sigma^2\bigr)\bigl[\exp\bigl(C_{\ln}(\mathbf{h})\bigr)-1\bigr] \\ &= \exp\bigl(2m+2\sigma^2\bigr)\bigl\{1-\exp\bigl[-\gamma_{\ln}(\mathbf{h})\bigr]\bigr\}. \end{aligned} \tag{19}$$

Concerning the conditional variogram, (18) has to be modified as follows:

$$\begin{aligned}\gamma_y(\mathbf{h}) &= \frac{1}{2}\frac{\sum_{p=0}^{+\infty}\bigl[1-\frac{\gamma_{\ln}(\mathbf{h})}{\sigma^2}\bigr]^p \int_{\xi}^{+\infty}\int_{\xi}^{+\infty}(e^{m+\sigma t}-e^{m+\sigma t'})^2 H_p(t)H_p(t')g(t)g(t')\,dt\,dt'}{\sum_{p=0}^{+\infty}\bigl[1-\frac{\gamma_{\ln}(\mathbf{h})}{\sigma^2}\bigr]^p \int_{\xi}^{+\infty}\int_{\xi}^{+\infty} H_p(t)H_p(t')g(t)g(t')\,dt\,dt'} \\ &= e^{2m+2\sigma^2}\frac{\sum_{p=0}^{+\infty}\bigl[1-\frac{\gamma_{\ln}(\mathbf{h})}{\sigma^2}\bigr]^p\bigl\{S_{0p}(\xi)\sum_{q=0}^{+\infty}\frac{(-2\sigma)^q}{\sqrt{q!}}S_{qp}(\xi)-e^{-\sigma^2}\bigl[\sum_{q=0}^{+\infty}\frac{(-\sigma)^q}{\sqrt{q!}}S_{qp}(\xi)\bigr]^2\bigr\}}{\sum_{p=0}^{+\infty}\bigl[1-\frac{\gamma_{\ln}(\mathbf{h})}{\sigma^2}\bigr]^p S_{0p}^2(\xi)} \end{aligned} \tag{20}$$

with $\xi = \frac{\ln(y)-m}{\sigma}$. The second equality in (20) relies on the following identity (Chilès and Delfiner 1999, p. 641)

$$\exp(\sigma t) = \exp\bigl(\sigma^2/2\bigr)\sum_{q=0}^{+\infty}\frac{(-\sigma)^q}{\sqrt{q!}}H_q(t). \tag{21}$$

In Fig. 13, the conditional variogram γ_y is plotted as a function of the prior variogram γ, for several values of the threshold y (0 and the deciles of the lognormal distribution) and logarithmic variance σ^2. As for Fig. 11, it is observed that the shape of the conditional variogram differs from that of the prior variogram and that a hole effect appears for large threshold values, even if the prior variogram is a non-decreasing function of the distance. Furthermore, unlike the Gaussian case, the conditional variogram may take values greater than the prior variogram, which is a manifestation of a proportional effect (Manchuk et al. 2009): the variability in high-value areas (above threshold y) is greater than that of low-value areas.

These results prove that, when a random field is known through a preferential sampling pattern, the sample variogram is an unbiased estimate of the conditional

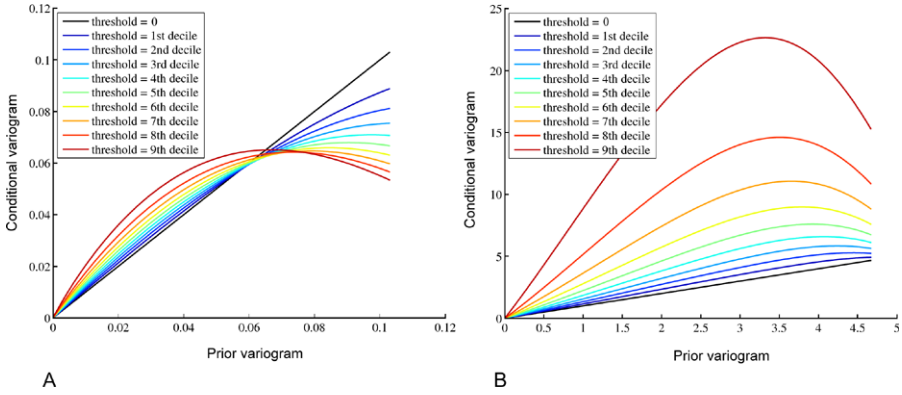

Fig. 13 Conditional variogram as a function of the prior variogram (stationary lognormal random field with logarithmic mean equal to 0 and logarithmic variance equal to (**A**), 0.09 and (**B**), 1.00)

variogram, but may be a biased estimate of the prior variogram. The knowledge of how such a preferential sampling has been designed (in the above examples, by discarding the data points where the random field takes values below a given threshold) is essential in order to correct for the bias.

References

Chilès JP, Delfiner P (1999) Geostatistics: modeling spatial uncertainty. Wiley, New York

Davis MW (1987) Production of conditional simulations via the LU triangular decomposition of the covariance matrix. Math Geol 19(2):91–98

Deutsch CV, Frykman P, Xie YL (1999) Declustering with seismic or "soft" geologic data. In: Report one 1998/1999. Centre for Computational Geostatistics, University of Alberta

Diggle PJ, Menezes R, Su TL (2010) Geostatistical inference under preferential sampling. J R Stat Soc, Ser C, Appl Stat 59:191–232

Dubrule O, Kostov C (1986) An interpolation method taking account inequality constraints: I—Methodology. Math Geol 18(1):33–51

Emery X (2006) A disjunctive kriging program for assessing point-support conditional distributions. Comput Geosci 32(7):965–983

Emery X (2008) A turning bands program for conditional co-simulation of cross-correlated Gaussian random fields. Comput Geosci 34(12):1850–1862

Emery X, Lantuéjoul C (2006) TBSIM: a computer program for conditional simulation of three-dimensional Gaussian random fields via the turning bands method. Comput Geosci 32(10):1615–1628

Emery X, Ortiz JM (2005) Histogram and variogram inference in the multigaussian model. Stoch Environ Res Risk Assess 19(1):48–58

Emery X, Ortiz JM (2007) Weighted sample variograms as a tool to better assess the spatial variability of soil properties. Geoderma 140(1–2):81–89

Emery X, Carrasco P, Ortiz J (2004) Geostatistical modelling of solubility ratio in an oxide copper deposit. In: Magri E, Ortiz J, Knights P, Henríquez F, Vera M, Barahona C (eds) 1st international conference on mining innovation. Gecamin Ltd, Santiago, Chile, pp 226–236

Goovaerts P (1997) Geostatistics for natural resources evaluation. Oxford University Press, New York

Guan Y, Afshartous DR (2007) Test for independence between marks and points of marked point processes: a subsampling approach. Environ Ecol Stat 14(2):101–111

Hu LY, Lantuéjoul C (1988) Recherche d'une fonction d'anamorphose pour la mise en œuvre du krigeage disjonctif isofactoriel gamma (Search for an anamorphosis function for the implementation of isofactorial gamma disjunctive kriging). Sci Terre Sér Inf Geol 28:145–173

Lantuéjoul C (2002) Geostatistical simulation: models and algorithms. Springer, Berlin
Leuangthong O, Deutsch CV (2003) Stepwise conditional transformation for simulation of multiple variables. Math Geol 35(2):155–173
Mallet JL (1980) Régression sous contraintes linéaires. Application au codage des variables aléatoires (Regression under linear constraints. Application to the coding of random variables). Rev Stat Appl 38(1):57–68
Manchuk JG, Leuangthong O, Deutsch CV (2009) The proportional effect. Math Geosci 41(7):799–816
McKay AT (1934) Sampling from batches. J R Stat Soc 1(Suppl):207–216
Olea RA (2007) Declustering of clustered preferential sampling for histogram and semivariogram inference. Math Geol 39(5):453–467
Parkinson GA, Bhappu RB (1995) The sequential copper analysis method—geological, mineralogical, and metallurgical implications. In: SME annual meeting, Denver
Pyrcz MJ, Deutsch CV (2003) Declustering and debiasing. In: Searston S (ed) Newsletter 19, October 2003. Geostatistical Association of Australasia, Melbourne
Razavizadeh H, Afshar MR (2008) Leaching of Sarcheshmeh copper oxide ore in sulfuric acid solution. Miner Metall Process 25(2):85–90
Richmond A (2002) Two-point declustering for weighting data pairs in experimental variogram calculation. Comput Geosci 28(2):231–241
Rivoirard J (1994) Introduction to disjunctive kriging and non-linear geostatistics. Oxford University Press, Oxford
Verly G (1983) The multigaussian approach and its applications to the estimation of local reserves. Math Geol 15(2):259–286
Yeo GF, Milne RK (1991) On characterizations of beta and gamma distributions. Stat Probab Lett 11:239–242